IEC-128

STATUS REPORT OF SUBGROUP 16 OF THE NEANSC WORKING PARTY ON INTERNATIONAL EVALUATION COOPERATION†

C. Y. Fu (coordinator) and D. C. Larson (monitor)
Oak Ridge National Laboratory, Oak Ridge, TN, USA

May. 5, 1995

1. INTRODUCTION

The purpose of this subgroup is to recommend a set of consistent level density formalisms and parameters for the isotopes of structural materials. Top priority has been given to residual nuclides required in ^{52}Cr, ^{56}Fe, and ^{58}Ni cross section calculations below 20 MeV.

Since the May 1994 meeting of the Working Party, the membership of the subgroup has been expanded to include Su Zongdi of Chinese Nuclear Data Center, Beijing, China and R. Capote Roy of Center of Applied Studies for Nuclear Development, Havana, Cuba. The coordinator has had collaboration from these two new members and from A. Mengoni and A. Zelenetsky (a colleague of A. Ignatyuk).

Level-density formulas examined are Gilbert-Cameron[1] (G-C), Back-Shifted Fermi Gas[2] (BSFG), and the Generalized Super-Fluid Model[3,4] (GSM). These are included in the TNG code as options so that their effects on calculated cross sections and particle emission spectra can be isolated.

2. NEW CALCULATION FOR ^{58}Ni

A new calculation for the ^{58}Ni cross sections was made (1) to account for a new evaluation of s-wave level spacing D_0 for ^{55}Fe, (2) to account for recently available (n,α) cross sections, and (3) to get a plausible set of G-C level-density parameters for ^{58}Ni, ^{58}Co, and ^{55}Fe as a benchmark for subsequent comparisons with the other two level-density formulas. The calculation was done using the TNG code. All model parameters other than level densities for the binary channels were fixed to isolate the level density effects.

a. D_0 for ^{55}Fe

Among the level densities required for calculating the binary cross sections, the only measured D_0 available is for ^{55}Fe. This D_0 value was fixed at 14.4 keV, based on the analysis of Z. Zhao and Z. Su of CNDC using the resonance parameters evaluated by F. G. Perey and C. M. Perey. The Fermi-gas a was derived from D_0 using:

†The U. S. part of this international collaboration was sponsored by Office of Energy Research, Division of Nuclear Physics, U. S. Department of Energy, under contract DE-AC05-84OR21400 with Martin Marietta Energy Systems, Inc.

$$U = E - U_0, U = at^2, \sigma^2 = (6/\pi^2)a\langle m^2\rangle t, \langle m^2\rangle = 0.24A^{2/3},$$

where E is the excitation energy and U_0 is the pairing energy correction of G-C, taken here as 1.54 MeV.

In the TNG code, the required input for G-C are a, $\langle m^2\rangle$, and E_0 for the Fermi gas part. The parameters (energy shift E_0, temperature T, and tangential point E_x) for the constant temperature part of G-C are determined automatically in TNG from input for the Fermi gas part and the discrete levels. The energy of the highest discrete level is called E_c. If $\langle m^2\rangle$ is not given, TNG takes the formula above as default.

The effective excitation energy U is defined differently in the BSFG and the GSM formalas to be given below.

b. Fit to ^{58}Ni cross sections

The a values for ^{58}Ni and ^{58}Co were adjusted via a series of TNG calculations to fit (n,n'), (n,p), and (n,α) cross sections using G-C. Since no other parameters were adjusted, the fit is not optimal. However, it is important to note that once the a value for ^{55}Fe is fixed, there can only be one set of a's possible in the fit. It is shown in Section 5 that an independent fit to the same set of cross sections by Zelenetsky[5] starting with a much larger D_0 for ^{55}Fe ended with a very different set of level density parameters.

The resulting G-C parameters are shown in Table 1, where the BSFG and GSM parameters described below are also listed for comparison.

The resulting cross sections are shown in Fig. 1. Experimental cross sections are not shown, but it is sufficient for our purpose here to note that the calculated values agree with 'evaluated' data to about 10%. (H. Vonach is presently evaluating the ^{58}Ni(n,α) data using Bayes theorem).

3. COMPARISON WITH BACK-SHIFTED FERMI GAS

The effects of the shape difference between BSFG and G-C on calculated cross sections and particle emission spectra are studied. The BSFG a and the shift Δ for each of the binary residual nuclides are obtained by fitting BSFG to G-C determined above at E_c and E_x.

The resulting BSFG/G-C ratios shown in Fig. 2 are unity at E_c and E_x. The difference between BSFG and G-C below E_x is the difference between a Fermi gas formula and a constant temperature formula. While the difference between BSFG and G-C above E_x is the difference between two Fermi gases using different a's and different energies ($U-\Delta$ and $U-U_0$). The BSFG parameters are also listed in Table 1. Note E_x is rather close to the neutron binding energy.

The spin cutoff factor in BSFG used here is given by

$$\sigma^2 = 0.0150A^{5/3}t, U - \Delta = at^2 - t$$

The effects of this different spin cutoff factor on cross sections and particle emission spectra have been determined to be much smaller than the shape effects being addressed in this report.

The impacts of the level-density shape differences between BSFG and G-C are shown in Fig. 3 for cross sections and Fig. 4 for particle emission spectra for an incident energy of 20 MeV.

From Fig. 3, it is seen that the BSFG/G-C ratios for (n,α) have a relative minimum at 8 MeV. For this incident energy, outgoing neutrons see a larger BSFG level density (Fig. 2) than outgoing alphas do. For incident energies greater than 14 MeV, the situation is reversed and the BSFG (n,α) gets larger.

The correlation between the particle emission spectra shown in Fig. 4 and the level densities shown in Fig. 2 is rather complicated because the results shown in Fig. 4 are not only related to the level-density differences shown in Fig. 2 but also to the cross sections shown in Fig. 3 and the tertiary-reaction contributions. For example, neutron emission below 4 MeV for BSFG is larger because the BSFG (n,pn), the dominant low-energy neutron emitter, is larger. And neutron emission for BSFG around 10 MeV is reduced because the BSFG (n,n') cross section is reduced.

4. COMPARISON WITH GENERALIZED SUPER-FULID MODEL

The effects of the shape difference between GSM and G-C on calculated cross sections and particle emission spectra are studied. The GSM asymptotic a and the shift δ for each of the binary residual nuclides are obtained by fitting GSM to G-C determined above at E_c and E_x.

The resulting GSM/G-C level density ratios are shown in Fig. 5. The GSM/G-C ratios are similar in characteristics to BSFG/G-C shown in Fig. 2. Because the shell corrections in GSM for ^{58}Ni, ^{58}Co, and ^{55}Fe are all negative, the Fermi gas parameters a in all three cases increase with excitation energies. This explains the smaller difference between GSM and G-C than between BSFG and G-C. The GSM parameters are also listed in Table 1.

Note that the spin cutoff factor in GSM is the same as used above for G-C, but U is defined differently:

$$U = E - E_{cond} + n\Delta_0 + \delta, \Delta_0 = 12A^{-1/2}$$

where A is the mass number, n = 0, 1, 2 for even-even, odd-A, and odd-odd nuclide. E_{cond} is the condensation energy in the model calculated from other input parameters. $E_{cond} - n\Delta_0$ is similar to the pairing correction of G-C. Another input parameter is the shell correction. Values of this correction were obtained from the HERMES code of Mengoni[4]. These are also listed in Table 1.

The impacts of the level-density shape differences between GSM and G-C are shown in Fig. 6 for cross sections and Fig. 7 for particle emission spectra for an incident energy of 20 MeV. The super-fluid region has no impact here because this region lies below E_c.

From Fig. 6, it is seen that the GSM/G-C ratios for (n,α) have a relative maximum at 8 MeV. For this incident energy, outgoing neutrons see a smaller GSM level density (Fig. 5) than outgoing alphas do. For incident energies greater than 12 MeV, the situation is reversed and the GSM (n,n') gets larger.

The behavior in the particle emission ratios for GSM/G-C shown in Fig. 7 are reversed from that of BSFG/G-C shown in Fig. 4. For example, neutron emission below 4 MeV

for GSM is smaller because the GSM (n, pn) is smaller. And neutron emission for GSM around 10 MeV is larger because the GSM (n, n') cross section is larger.

5. COMPARISONS WITH ZELENETSKY

An independent calculation for ^{58}Ni by Zelenetsky[5] using GSM is briefly describely here. He also started with an available D_0 for ^{55}Fe and considered the newly available (n, α) data to determine the level-density parameters for ^{58}Ni and ^{58}Co. The resulting binary cross sections are rather similar to those shown in Fig. 1 (considering the differences in optical model parameters and pre-equilibrium models). The interesting part of this work is that he started with a ^{55}Fe D_0 value of 20.4 keV (compared with 14.4 keV used in Section 2). This larger D_0 led to smaller asymptotic a's for all binary residual nuclides, also shown in Table 1. The differences between the shell corrections used by Zelenetsky and those used in Section 4 are due to different sources for these quantities. In neither cases are they adjustable parameters.

Further communication with Zelenetsky should include comparisons for particle emission spectra for several incident energies, probably comparisons with some experimental data also.

6. OTHER PROGRESS

Su has compared the s-wave level spacings in three libraries (China, Italy, and Russia). His conclusion from this comparison and from the Chinese analysis is that the uncertainties in these spacings are over 20% in general, arising mainly from differences in the data sources and methods of analysis. For the better measured targets, such as ^{56}Fe and ^{56}Ni (level densities for ^{57}Fe and ^{59}Ni), the uncertainties are still as large as 10%.

Capote has made combinatorial calculations for level densities of ^{58}Co, ^{58}Fe, and ^{58}Ni. The calculations started with quasi-particle levels to include pairing and shell effects. The results were compared with those from BSFG and GSM. The shapes of the combinatorial results favor GSM.

Mengoni[4] has developed a new semi-empirical model of level densities using an approach similar to the high-energy part of GSM. Data required for the shell corrections can be obtained from the code HERMES. The model appears to describe the existing D_0 data better than others available. However, the model lacks a description for the discrete levels. One way to use the predictions in this model for a blind calculation is to preserve the predicted D_0 and adjust the asymptotic a and an energy shift (independent of the pairing correction as in GSM) to fit the cumulative number of discrete level at E_c. Another way is to use a constant temperature formula for the low energy part similar to G-C.

7. PRELIMINARY OBSERVATIONS

The importance of understanding the impacts of the differences among level density formalisms on calculated cross sections and particle emission spectra needs not be emphasized. In this section, we comment on the strengths and weaknesses of each model studied in this report.

The fact that G-C has a constant temperature part for low excitation energies and a

Fermi gas part for higher energies is a strength, not a weakness, at least for ^{52}Cr, ^{56}Fe, and ^{58}Ni cross-section calculations. The numbers of discrete levels in the residual nuclides required in these calculations are rather abundant such that the level densities at E_c are relatively well defined. The constant temperature part of the model requires no input parameters. Secondly, the Fermi gas part may be used to fit the D_0 values without the disruption of an arbitrary energy shift (in addition to the pairing energy shift) that has no physical meaning in the Fermi gas model. The original argument by G-C for introducing the constant temperature part is to compensate for the low-energy collective levels not included in the Fermi gas model.

The weakness of G-C is in its shell correction that is included in a constant a for all excitation energies. At high excitation energies, in which particles far below the Fermi surface get excited, the shell correction should approach zero. This dwindling shell correction is treated in GSM, one of its strengths.

GSM has the strongest physics in both pairing corrections and shell corrections. However, the fact that GSM still needs an arbitrary energy shift to fit both D_0 at the neutron binding energy and the discrete level region, at least for the nuclides considered here, is a disappointment. It is seen from Fig. 7 that GSM/G-C is smaller than unity above E_x. This means the effects of the shift factor overpower the effects of the dwindling shell corrections.

For the same reason, the back shift used in BSFG has no physical basis. Like the G-C, the shell effects in BSFG are accounted for in a constant a, a second weakness.

As a preliminary recommendation, BSFG should be restricted to calculations below about 14 MeV. GSM is the strongest in physics but suffers from less applications. In cases the energy shift used in GSM is large, the effects of the shift tends to destroy the desirable energy-dependent shell corrections. A possible remedy is to use the shift in an energy-dependent manner as the shell correction.

This status report has not yet been reviewed by members of subgroup 16 prior to its presentation at the May 1995 NEANSC Evaluation Cooperation Meeting.

8. REFERENCES

1. A. Gilbert and A. G. W. Cameron, *Can. J. Phys.* **13**, 1446 (1965).
2. W. Dilg, W. Schantl, H. Vonach, and M. Uhl, *Nucl. Phys.* **A217**, 269 (1973).
3. A. V. Ignatyuk, J. L. Weil, S. Raman, and S. Kahane, *Phys. Rev.* **C47**, 1504 (1993).
4. A. Mengoni and Y. Nakajima, *J. Nucl. Sci. Tech.* **31**, 151 (1994).
5. A. Zelenetsky, Institute of Atomic Energetics, Obninsk, Russia, Private Communication (1995).

Table 1. Level-density parameters

		Ni-58	Co-58	Fe-55
Gilbert-Cameron				
	a	6.200	7.300	7.256
	U_0	2.470	0	1.540
Back-Shifted Fermi Gas				
	a	5.322	6.210	6.188
	Δ	0.210	-1.910	-0.210
Generalized Super-fluid Model				
	asymptotic a	6.496	7.266	7.576
	δ	2.680	1.468	1.530
	shell corr.	-4.037	-2.318	-2.977
Generalized Super-fluid Model of Zelenetsky				
	asymptotic a	5.68	5.33	4.80
	δ	0.15	0.16	0.08
	shell corr.	-2.40	-2.06	-2.42

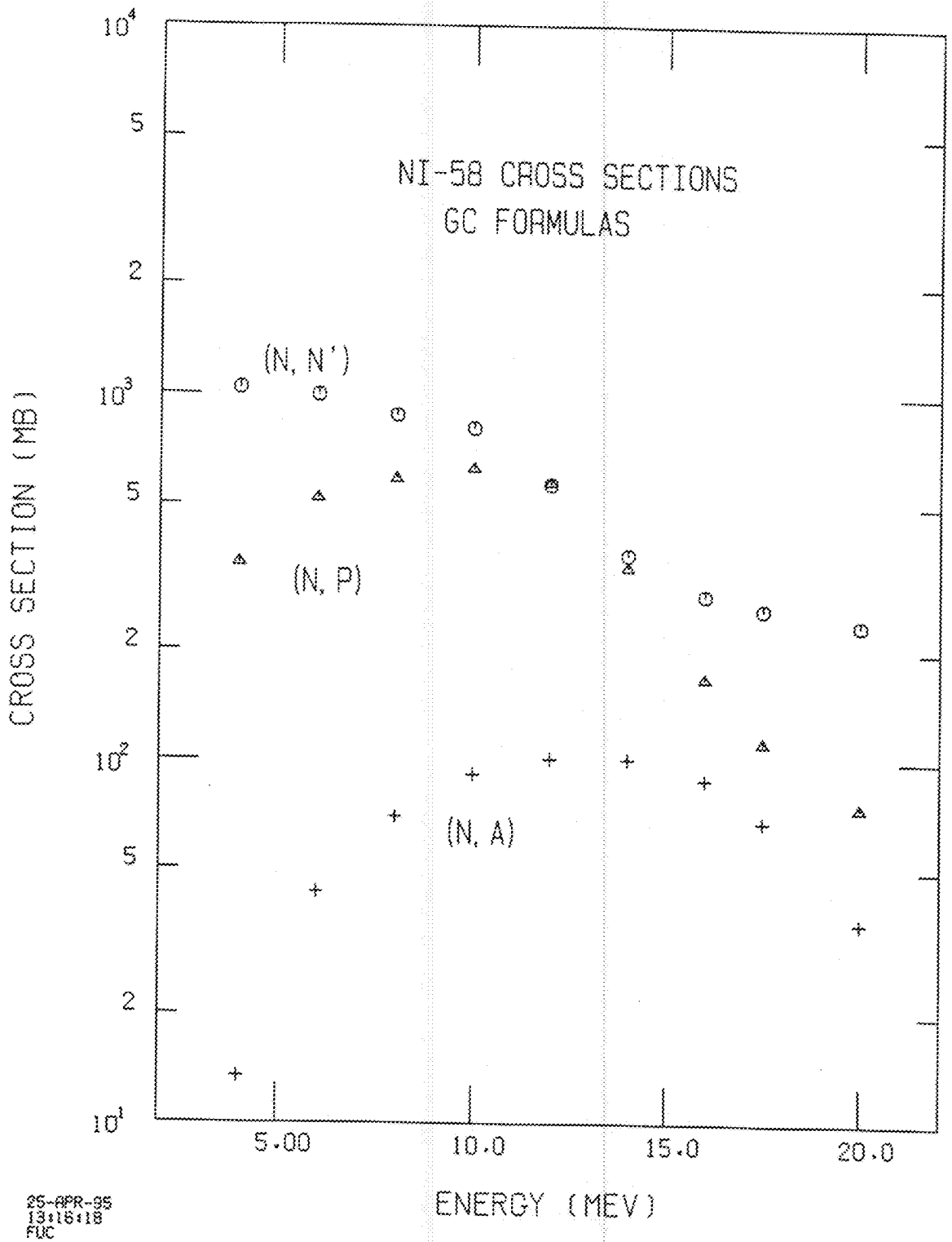
NI-58 CROSS SECTIONS
GC FORMULAS
CROSS SECTION (MB)
ENERGY (MEV)
(N, N')
(N, P)
(N, A)
10^4
5
2
10^3
5
2
10^2
5
2
10^1
5.00
10.0
15.0
20.0
25-APR-95
13:15:18
FUC

Fig. 1.

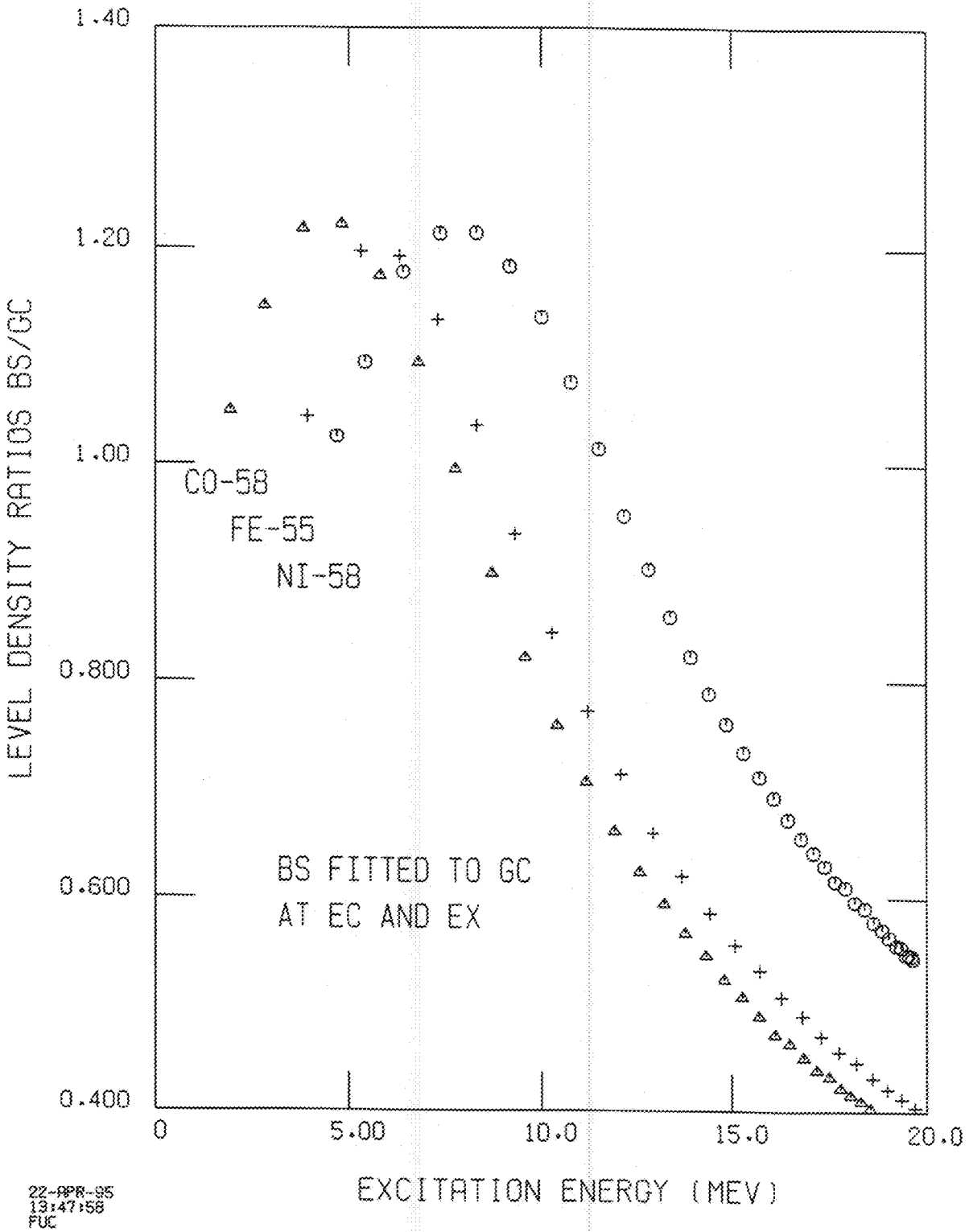
1.40
1.20
1.00
0.800
0.600
0.400
LEVEL DENSITY RATIOS BS/GC
CO-58
FE-55
NI-58
BS FITTED TO GC
AT EC AND EX
0
5.00
10.0
15.0
20.0
EXCITATION ENERGY (MEV)
22-APR-95
13:47:58
FUC

Fig. 2.

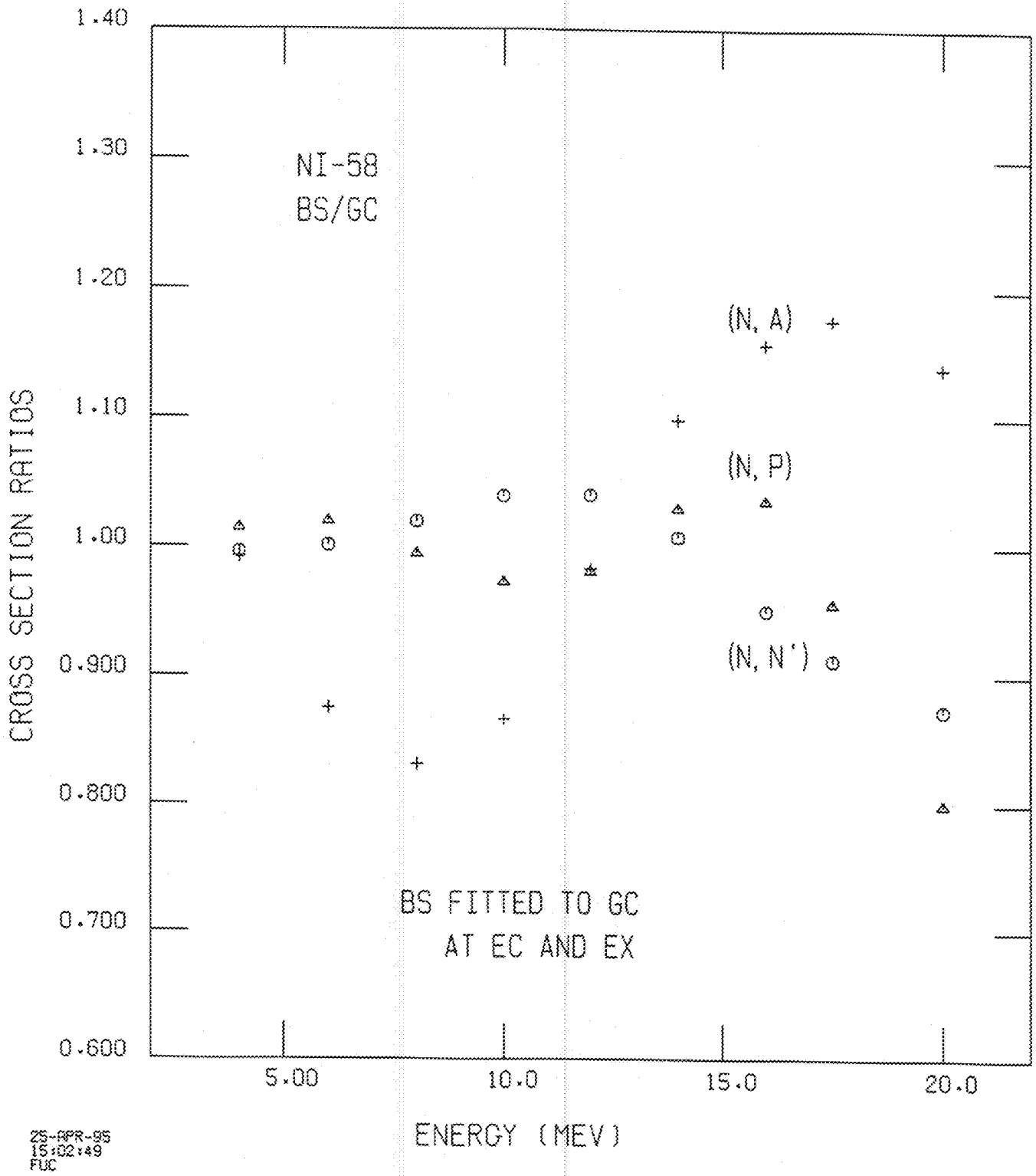
NI-58
BS/GC
(N, A)
(N, P)
(N, N')
BS FITTED TO GC
AT EC AND EX
CROSS SECTION RATIOS
ENERGY (MEV)
1.40
1.30
1.20
1.10
1.00
0.900
0.800
0.700
0.600
5.00
10.0
15.0
20.0
25-APR-95
15:02:49
FUC

Fig. 3.

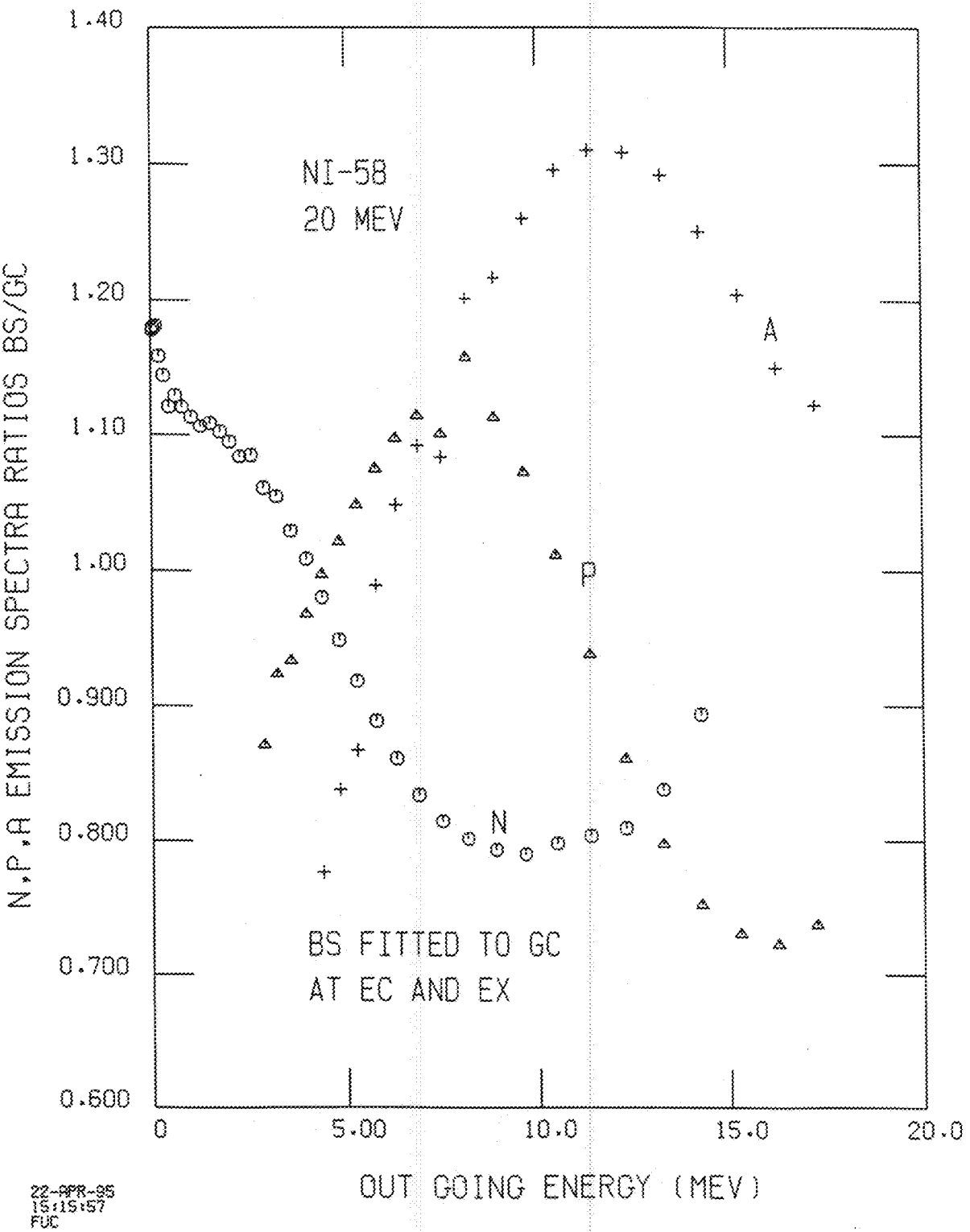
1.40
1.30
1.20
1.10
1.00
0.900
0.800
0.700
0.600
N,P,A EMISSION SPECTRA RATIOS BS/GC
NI-58
20 MEV
A
P
N
BS FITTED TO GC
AT EC AND EX
0
5.00
10.0
15.0
20.0
OUT GOING ENERGY (MEV)
22-APR-85
15:15:57
FUC

Fig. 4

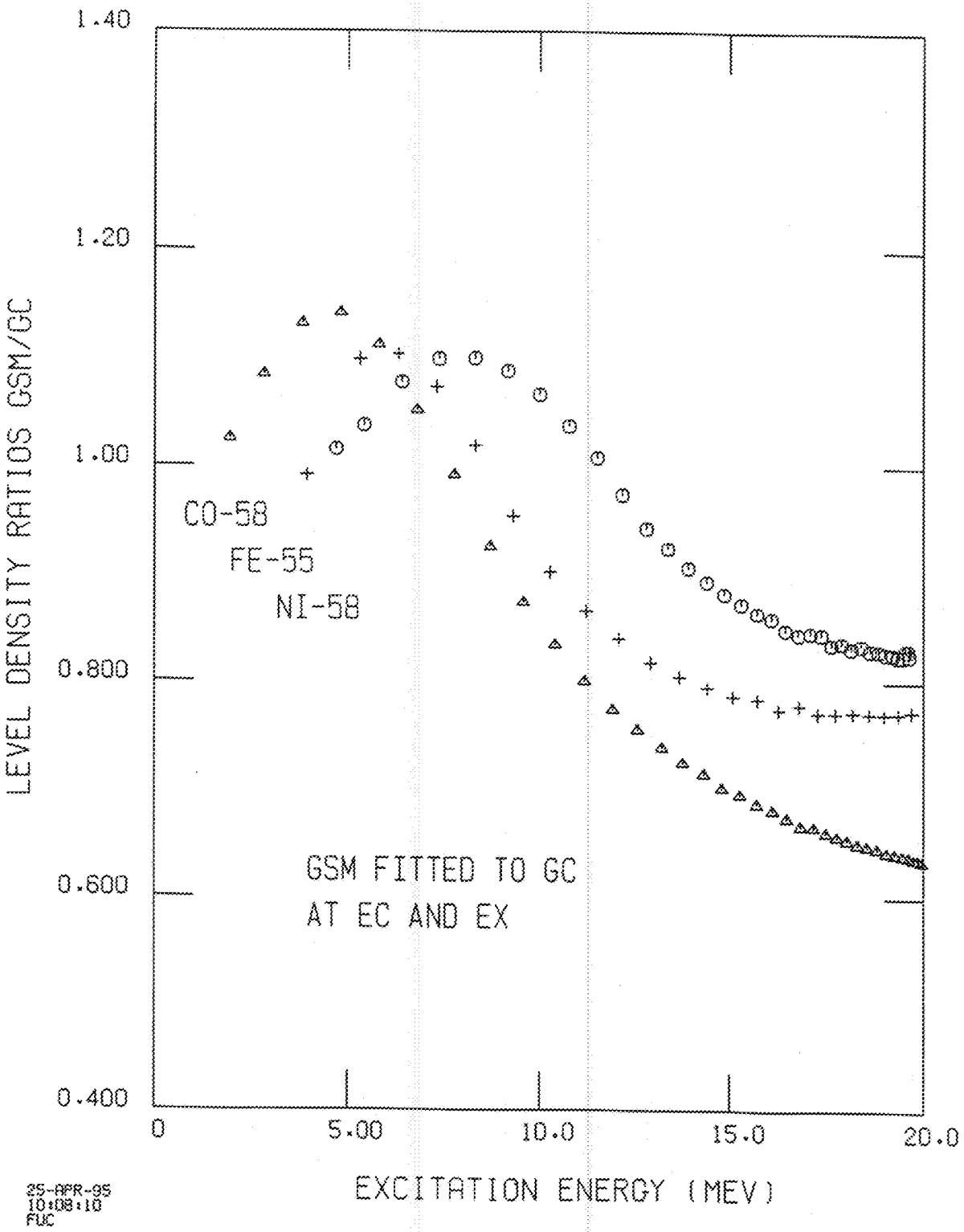
1.40
1.20
1.00
0.800
0.600
0.400
LEVEL DENSITY RATIOS GSM/GC
CO-58
FE-55
NI-58
GSM FITTED TO GC
AT EC AND EX
0
5.00
10.0
15.0
20.0
EXCITATION ENERGY (MEV)
25-APR-95
10:08:10
FUC

Fig. 5

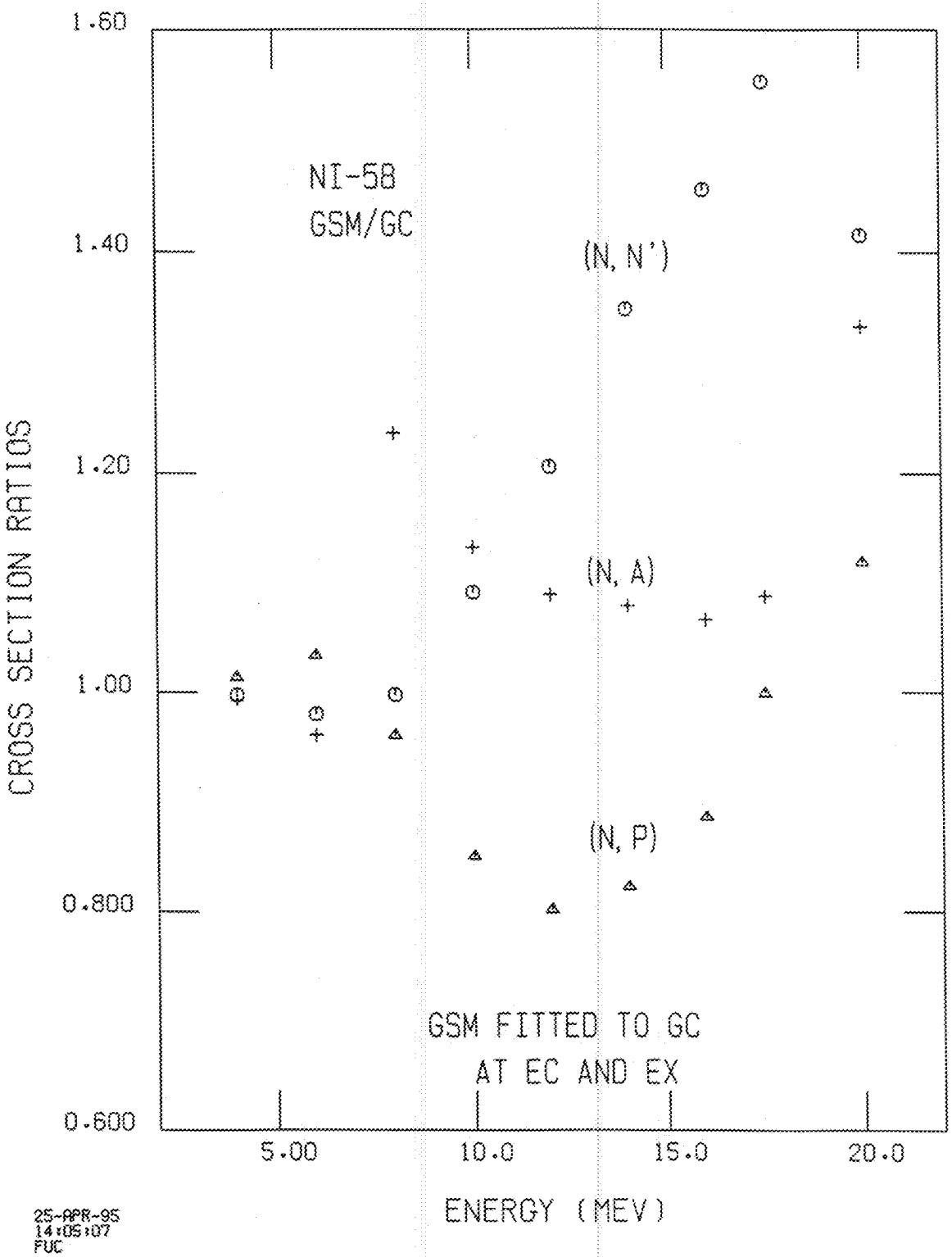
NI-58
GSM/GC
(N, N')
(N, A)
(N, P)
GSM FITTED TO GC
AT EC AND EX
CROSS SECTION RATIOS
ENERGY (MEV)
1.60
1.40
1.20
1.00
0.800
0.600
5.00
10.0
15.0
20.0
25-APR-95
14:05:07
FUC

Fig. 6

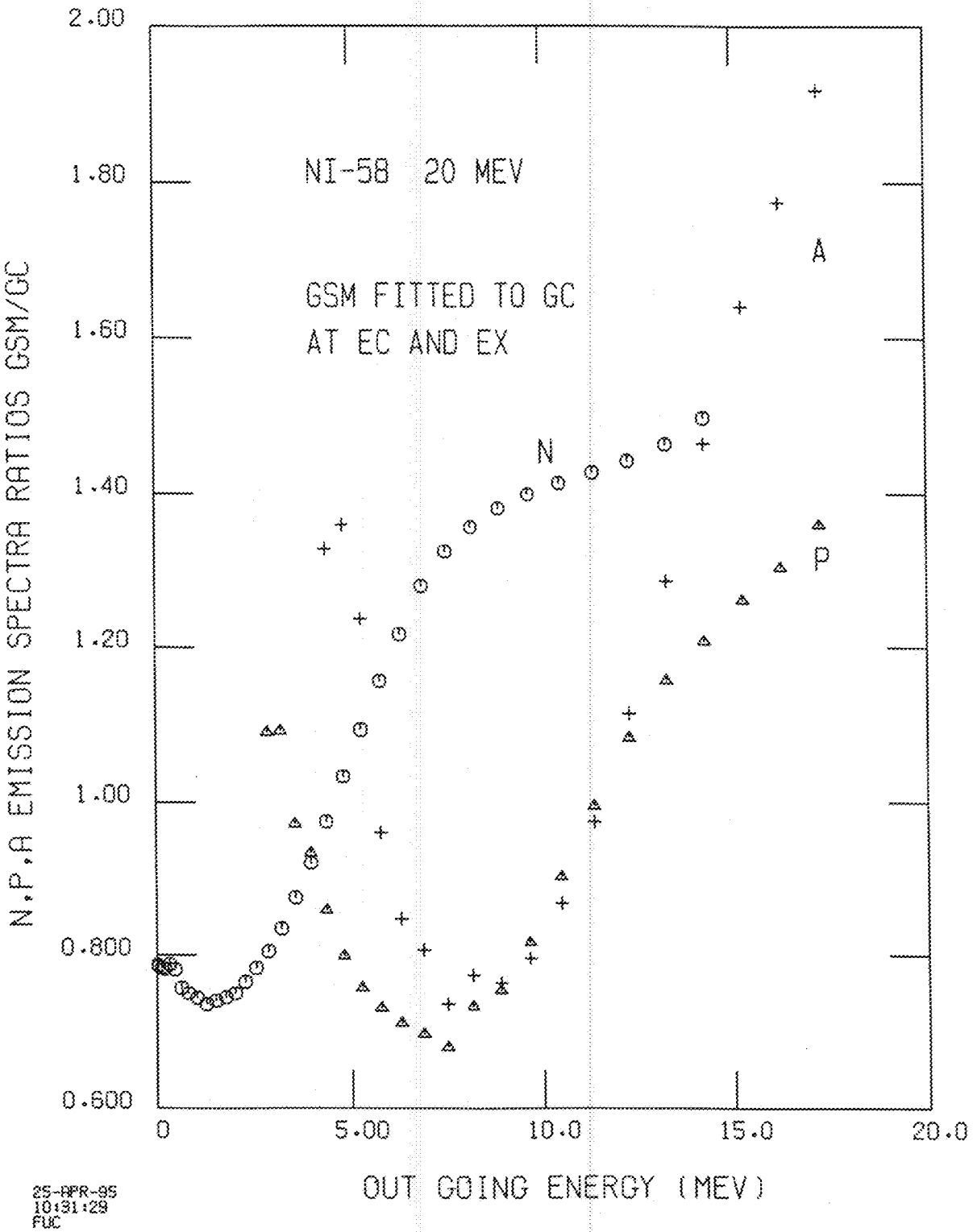
NI-58 20 MEV
GSM FITTED TO GC
AT EC AND EX
N
P
A
N.P.A EMISSION SPECTRA RATIOS GSM/GC
OUT GOING ENERGY (MEV)
2.00
1.80
1.60
1.40
1.20
1.00
0.800
0.600
0
5.00
10.0
15.0
20.0
25-APR-95
10:31:29
FUC

Fig. 7